NATIONAL ADVISORY COMMITTEE FOR AERONAUTICS

TECHNICAL NOTE 2825

A COMPARATIVE EXAMINATION OF SOME MEASUREMENTS OF AIRFOIL SECTION LIFT AND DRAG AT SUPERCRITICAL SPEEDS

By Gerald E. Nitzberg and Stewart M. Crandall

Ames Aeronautical Laboratory
Moffett Field, Calif.

Washington
November 1952

1F

NATIONAL ADVISORY COMMITTEE FOR AERONAUTICS

TECHNICAL NOTE 2825

A COMPARATIVE EXAMINATION OF SOME MEASUREMENTS OF AIRFOIL SECTION LIFT AND DRAG AT SUPERCRITICAL SPEEDS

By Gerald E. Nitzberg and Stewart M. Crandall

SUMMARY

A study was made of the lift and drag characteristics, as determined from wind-tunnel tests, of a number of airfoil sections at supercritical Mach numbers.

Semiempirical correlations of supercritical drag data were made for a family of symmetrical airfoils and for several series of cambered airfoils at small and moderate angles of attack. The correlations are of pressure-drag rise per unit chord length as a function of Mach number. For the airfoils considered, there is an essentially unique shape of the drag-rise curve when the angle of attack is that for maximum drag-divergence Mach number. The primary effect of changing the airfoil shape apparently is to change the Mach number at which the drag rise begins. No means have been devised for applying these results to the prediction of supercritical drag characteristics.

The lift study consisted primarily of an examination of the separate normal-force components of the upper and lower surfaces of several airfoil sections. One of the most significant observations to be made concerning the lift data studied is that, at moderate positive angles of attack and in the range of Mach numbers for which supersonic flow occurred over only the upper surface, there appeared a marked change in the rate of variation with $(1 - M^2)^{-1/2}$ of the component of the normal-force coefficient contributed by the lower surface as the drag-divergence Mach number was exceeded. This change was most abrupt for thicker sections and is the primary cause of the loss of lift at supercritical speeds.

INTRODUCTION

Theoretical treatment of the flow of a compressible fluid about an airfoil section at supercritical, subsonic speeds in a rigorous manner has met with great difficulty. Furthermore, the importance of shock-wave boundary-layer interaction in transonic flows might invalidate any

theory which assumes the existence of inviscid flow. Consequently, experiment has been the principal source of information concerning the behavior of airfoil sections at supercritical, subsonic Mach numbers. Section force coefficients for a large number of airfoil sections have been measured at supercritical Mach numbers. These data indicate that between airfoil sections there are important differences in the variation with Mach number, at constant angle of attack, of lift and drag coefficients. For a given airfoil section differences exist between the variation of force characteristics with Mach number at various angles of attack. One purpose of this report is to point out some systematic trends in the lift- and drag-coefficient variation with Mach number for a number of families of airfoil sections at supercritical free-stream Mach numbers.

The flow changes associated with the drag rise of airfoil sections at supercritical, subsonic speeds were studied in reference 1. It was found that the initial supercritical drag rise was primarily an increase in pressure drag due to the variation with Mach number of the airfoil pressure distribution over the region surrounding the sonic point. A means for comparing the transonic potential flow fields about thin wings having similar shapes but different thickness-chord ratios has been presented in the form of similarity rules (e.g., references 2 and 3). In this report one form of these similarity rules is applied to the section drag data measured for a family of airfoils at supercritical, subsonic Mach numbers. The shortcomings of these rules are discussed and a semiempirical correlation of drag data is presented.

In reference 1, it was suggested that the lift break for airfoil sections at supercritical, subsonic speeds and at positive angles of attack may be due primarily to pressure-distribution changes on the lower surface. The loss in lift is not produced by the pressure alterations in the portion of the flow field (upper surface) in which supersonic velocities exist. The initial loss in lift results from lower-surface pressure-distribution changes which were tentatively attributed to effects of the large wake accompanying the supercritical drag rise. If this hypothesis is correct then, inasmuch as such wake effects are not included in the potential theory on which the transonic similarity rules are based, these rules would not be expected to be useful as a guide for directly correlating supercritical lift characteristics. The lift study in this report consists primarily of an examination of the separate lift components of the upper and lower surfaces of several airfoil sections.

NOTATION

c	chord of airfoil section
c_d	airfoil-section drag coefficient
$c_{d_{cr}}$	airfoil-section drag coefficient at critical Mach number
c_{d_p}	airfoil-section pressure-drag coefficient
Δc_d	increment of airfoil-section drag coefficient ($c_d - c_{d_{cr}}$)
c_l	airfoil-section lift coefficient
c_n	airfoil-section normal-force coefficient
c_{n_l}	normal-force coefficient of airfoil-section lower surface
c_{n_u}	normal-force coefficient of airfoil-section upper surface
K	transonic similarity parameter
K_{cr}	transonic similarity parameter for critical Mach number
M	free-stream Mach number
M_{cr}	critical Mach number
M_d	drag-divergence Mach number, free-stream Mach number at which $\frac{dc_d}{dM}$ has value of 0.1
M_k	correlation Mach number
M_β	Mach number at which sonic velocity is reached at airfoil crest (point on surface at which tangent to surface is in free-stream direction)
p_o	total pressure
q	free-stream dynamic pressure

t maximum thickness of airfoil section

x chordwise distance from airfoil leading edge

y ordinate of airfoil

α airfoil-section angle of attack

α_m angle of attack at which airfoil section has the highest drag-divergence Mach number

DATA AND SCOPE

The data used in this study were obtained from references 4, 5, 6, 7, and 8. The airfoil sections considered are both cambered and uncambered and are of the NACA four-digit series, five-digit series, and 6 series. No data on airfoil sections with deflected flaps, airfoil sections having reflexed camber lines, or airfoil sections designed for supersonic application are studied. The thickness-chord ratio of the airfoil sections considered ranges from 0.06 to 0.18.

The data presented in references 5 and 8 are from two-dimensional tests made in the Ames 1- by 3-1/2-foot high-speed wind tunnel and have been corrected for the effects of the tunnel walls by the methods presented in reference 9. For the Mach numbers to be considered, the Reynolds number of these tests was about 2 million. The data of references 4, 6, and 7 were obtained from tests of finite-span models in the DVL (2.7 meter diameter) high-speed wind tunnel. However, these models were equipped with end plates and the angles of attack were corrected to correspond to infinite span. Corrections were also applied to convert the experimental values to free-air conditions. The Reynolds number for these tests was about 6 million for the Mach numbers studied in this report.

The question arises as to the accuracy of the tunnel corrections which were applied to these wind-tunnel measurements made at high speeds, especially when there was high drag, flow separation, and a large wake. At Mach numbers lower than those at which the abrupt supercritical drag rise began (drag divergence), only the solid blockage of the models was important and the small size of the models relative to the wind-tunnel cross-section areas insured that the tunnel-wall corrections were small and predictable from theory. However, at higher Mach numbers, with the rapid increase in drag coefficient, the correction for the effects of the model wake became large. The effects of compressibility on the wake-blockage correction were determined by means of the Prandtl rule which may not be applicable. In fact, an

experimental study by Feldman (reference 10) shows that when there is a relatively large drag coefficient due to pressure drag the conventional tunnel-wall corrections are too small.[1] The Mach numbers shown in the figures of the present report may be in error by several percent which imposes a limitation on the usefulness of these data for quantitative analyses.

AIRFOIL-SECTION DRAG RISE AT SUPERCRITICAL SPEEDS

Transonic Similarity Rule

The transonic similarity rules (e.g., references 2 and 3) relate the transonic potential flow fields about thin bodies having similar aerodynamic shapes but different thickness-chord ratios. The condition necessary for a series of bodies to have similar aerodynamic shapes is

$$\frac{y/c}{t/c} = f(x/c) \tag{1}$$

The flows about two bodies having shapes such that equation (1) is satisfied are similar (i.e., represented by the same nondimensional potential-flow equation) when, according to reference 3, the condition

$$\left[\frac{M^2-1}{(M^2t/c)^{2/3}}\right]_1 = \left[\frac{M^2-1}{(M^2t/c)^{2/3}}\right]_2 = K \tag{2}$$

is met. Moreover, the pressure-drag coefficients of the two bodies (for the same value of K) are then related by

$$\left[\frac{M^{2/3}c_{d_p}}{(t/c)^{5/3}}\right]_1 = \left[\frac{M^{2/3}c_{d_p}}{(t/c)^{5/3}}\right]_2$$

[1] The theoretical blockage corrections applied by Feldman are based on the work of Thom (reference 11). Later analysis has led to some revisions of these theoretical corrections. However, these revisions do not affect significantly the results presented by Feldman.

For a family of similarly shaped bodies the pressure-drag coefficient is thus given by the relation

$$\frac{M^{2/3}c_{d_p}}{(t/c)^{5/3}} = F(K) \tag{3}$$

The basic assumptions made in the derivation of the transonic similarity rules are that the flow is inviscid and that the velocity at each point in the fluid is not far different from the local velocity of sound. The flows to be considered in this report (around airfoils at supercritical, subsonic speeds) are not entirely in accord with these assumptions. The flow about airfoil sections at supercritical speeds is influenced by the presence of shock-wave boundary-layer interaction. But the applicability of the similarity rule is more drastically curtailed by the fact that the drag rise of airfoils of moderate thickness-chord ratio or of thin airfoils at moderate angles of attack starts at free-stream Mach numbers substantially less than unity. Moreover, airfoil sections designed for subsonic speed applications have large disturbances at the blunt leading edges which produce stagnation points. On the other hand, the flow field is approximately potential for the initial portion of the supercritical drag-rise curve for which the viscous losses are generally small and essentially independent of Mach number. The initial supercritical drag rise is primarily an increase of pressure drag due to the change of pressure distribution in the region where the flow velocity is approximately sonic; therefore, it cannot be concluded a priori that the presence of a stagnation region and of shock-wave boundary-layer interaction obviates the usefulness of the similarity rules.

One form of the transonic similarity rules will now be tested by means of some experimental drag data for a family of symmetrical airfoil sections at zero angle of attack.

Correlation of Experimental Drag Data by Similarity Rules

In general, airfoil-section drag coefficients are determined from wake-survey or balance measurements and, consequently, include both skin friction and pressure drag. Since the transonic similarity rules apply to the pressure drag only, it is necessary to subtract the skin-friction drag from the measured drag. The drag of commonly used airfoil sections at small angles of attack and at subcritical Mach numbers is essentially independent of Mach number and due almost entirely to skin friction. At supercritical speeds, the skin-friction drag may be somewhat lower than at subcritical Mach numbers because of the increased chordwise extent of the favorable pressure gradient

over the forward portion of the airfoil and the increased stability of the laminar boundary layer (reference 12), which may cause the transition point to move rearward. However, because of the difficulty in estimating the value (probably small) of the decrease in skin-friction coefficient, it is assumed in the following correlation that the skin-friction drag coefficient at all supercritical Mach numbers is equal to the experimentally determined total airfoil-section drag coefficient at the critical Mach number. The remaining portion of the drag coefficient at supercritical Mach numbers is considered to be the pressure-drag coefficient, that is,

$$c_{d_p} \approx \Delta c_d = c_d - c_{d_{cr}}$$

High-speed drag data for symmetrical NACA four-digit-series airfoil sections of 6-, 9-, 12-, 15-, and 18-percent-chord thickness, each at 0° angle of attack, are presented in reference 4. Values of the parameter $\frac{M^{2/3}\Delta c_d}{(t/c)^{5/3}}$ calculated using the experimental data of reference 4 are plotted (fig. 1) against the parameter $\frac{M^2 - 1}{(M^2 t/c)^{2/3}}$ as suggested by one form of the transonic similarity rule. (See equation (3).) This method of plotting the data provides good correlation except for the 6-percent-thick section, and the maximum difference between the curve for this section and that for the 9-percent-thick section corresponds to a possible error in Mach number of only about 2 percent at a pressure drag coefficient of about 0.02.

The excellence of this correlation must be regarded as somewhat fortuitous because the form of the similarity parameter used happens to correlate the critical Mach numbers of this family of airfoil sections. This form of the parameter does not correlate the critical Mach numbers of ellipses or low-drag airfoils. From theoretical considerations it can be argued that there are two "natural" forms of the similarity parameter, that presented in equation (2) with the $M^{-4/3}$ factor either included or deleted. These two forms arise because M^2 either can be retained or set equal to 1 in the differential equation for transonic flow, the basic parameter being $(M^2 - 1)$. For the data presented in figure 1, retaining the factor $M^{-4/3}$ is essential to the correlation of critical Mach number; the other natural form of the similarity parameter does not provide good correlation of this supercritical drag data. In general, neither natural form of the similarity parameter provides good correlation of the critical Mach numbers of families of airfoils. Although the critical Mach number is not the Mach number at which force breaks occur, it is the lower limit of the transonic range. The degree of correlation of critical Mach number is a measure of the accuracy of the similarity rule for a given family of airfoils at Mach numbers substantially below 1.

In reference 8 the supercritical drag data for 16 cambered airfoils at zero angle of attack were correlated both empirically and according to a modified form of the transonic similarity rules. The airfoils considered had different thickness-chord ratios but all had the same camber line and hence were not similar. In an attempt to adjust for the dissimilarity in shape, the variable K was replaced by $K - K_{cr}$. Such a substitution would be consistent with the transonic theory if K_{cr} were constant; however, as was pointed out in the preceding paragraph, K_{cr} actually may not be constant for similar airfoils. This modification of the similarity parameter, which led to satisfactory correlation of the data considered, was somewhat arbitrary because the parameter K_{cr} (not constant for these airfoils) was adjusted to the actual critical Mach numbers. This application of the similarity rules indicates that forms of the similarity parameters which provide an accurate correlation of critical Mach number, even if these forms are synthetic, are useful for correlating the supercritical drag characteristics of airfoil sections.

The critical Mach number can be calculated with reasonable accuracy by means of potential theory plus the Kármán-Tsien compressibility correction. Thus it is possible to calculate critical Mach numbers and then select particular forms of the similarity parameter which are useful for a given family of airfoils. In deriving transonic similarity rules the assumption is made that velocity perturbations are small, which means that the Mach numbers throughout the flow field differ only slightly from unity. Hence factors such as M or M^2 are, to the accuracy of the theory, equal to 1 and can be inserted or deleted at will. It is thus apparent that there are an unlimited number of forms of the similarity parameters from which to choose one which correlates critical Mach numbers of a given family of airfoils.

Semiempirical Correlation of Experimental Drag Data

An alternative method for correlating drag data is suggested by the analysis of reference 1. In reference 1 the initial supercritical drag rise of an airfoil was related to two pressure-distribution changes:

1. At points ahead of the airfoil crest (the point on the airfoil at which the surface is tangent to the free-stream direction) for free-stream Mach numbers greater than the drag-divergence Mach number, the local Mach number was essentially constant for increasing free-stream Mach number. These constant local Mach numbers result in increasingly positive local pressure coefficients on the forward portion of the airfoil, and consequently an increase in drag coefficient, as the free-stream Mach number is increased beyond that for drag divergence.

2. The supersonic region behind the airfoil crest increases in chordwise extent as the free-stream Mach number is increased beyond that for drag divergence. This results in a decrease in pressure coefficient over the rear portion of the airfoil and hence an increase in drag coefficient.

Both these factors depend on the Mach number distribution over the airfoil section. This suggests relating the drag rise to the total pressure of the free stream rather than the dynamic pressure, that is, $\Delta(c_d\ q/p_o) = (c_d\ q/p_o)_M - (c_d\ q/p_o)_{M_{cr}}$. Accordingly, the data presented in figure 1 were plotted on curves of $\Delta(c_d\ q/p_o)$ versus M. It was observed that the curves for the several airfoils were similar. In order to illustrate the similarity, the curves were superposed by arbitrarily shifting the Mach number scale so that the increment in Mach number is measured from that Mach number M_k at which $\Delta(c_d\ q/p_o)$ equals 0.008 (fig. 2). Aside from the somewhat more rapid initial drag rise of the thickest airfoil section (possibly due to separation effects) the similarity is marked. The curves were matched at a point corresponding to a relatively large drag rise in order to minimize errors introduced by the assumption that above the critical Mach number the skin-friction coefficient is independent of Mach number.

For the NACA 0015 airfoil section, another set of measurements (reference 5) is also plotted on figures 1 and 2. These data were obtained at a Reynolds number of about 2 million as compared with a Reynolds number of about 6 million for the data from reference 4. The differences in these two sets of data are probably primarily due to Mach number errors (see section Data and Scope) rather than Reynolds number effects. The method of correlation used in figure 2 absorbs Mach number errors in the quantity M_k.

Data for other series of symmetrical airfoil sections of similar shape but different thickness-chord ratios were not available. In reference 8 are presented drag data for NACA 63-2XX, 64-2XX, 65-2XX, and 66-2XX airfoil sections at various angles of attack. For each group there are data for four thickness-chord ratios (0.06, 0.08, 0.10, and 0.12). Each of the airfoil sections of the above groups was cambered with an $a = 1.0$ type mean line for a design lift coefficient of 0.2. At 0° angle of attack the theoretical values for velocities over the upper surface of an airfoil with an $a = 1.0$ type mean line are uniformly greater than the velocities over the lower surface. It is therefore apparent that at this angle of attack the supercritical drag rise due to flow over the upper surface will begin at a lower Mach number than the drag rise caused by the flow over the lower surface. The angle of attack for which the drag rise due to the flow over each surface begins at the same Mach number ($\alpha = 0^\circ$ for symmetrical airfoils) is obviously that angle of attack α_m for which the initial drag rise

starts at the highest Mach number. For the afore-mentioned NACA 64-, 65-, and 66-series airfoil sections this angle of attack is about -2°. (The data for the NACA 63 series indicate a value of α_m closer to 0° than to -2° so for the sake of simplicity these sections will not be included in the correlations.) It might be expected that the data for these airfoils at -2° angle of attack would be comparable to those for the symmetrical NACA 00XX series at 0° angle of attack. The results of the analysis are presented in figure 3. No significant difference between the three airfoil groups is apparent. Furthermore, the faired curve drawn through these data is the same as that drawn through the data presented in figure 2.

Some additional data (reference 6) for cambered airfoils at the angle of attack (fortuitously $\alpha_m = -2^{\circ}$ again) for maximum drag-divergence Mach number are presented in figure 4. Each section had an NACA 230 mean line and the same thickness distribution as an NACA four-digit-series airfoil of equal thickness-chord ratio. For these cambered airfoils at the angle of incidence α_m the pressure distribution on the upper and lower surfaces differed markedly from each other; nevertheless, these data are in reasonable agreement with the faired curve obtained for the uncambered NACA four-digit-series airfoils at 0° angle of attack.

In reference 1, it was shown that the Mach number at which the abrupt supercritical drag rise begins is associated with that Mach number M_β for which sonic velocity is reached at the airfoil crest. Values of M_β calculated by applying the Prandtl-Glauert rule to the theoretical pressure distributions obtained from reference 13 are compared with values of M_k in the following table. If a systematic variation of $M_k - M_\beta$ with airfoil shape or thickness-chord ratio could be established it would be possible to predict the supercritical drag rise of other related airfoils. The tabulated values suggest that this Mach number increment varies with thickness-chord ratio and airfoil family. However, since this variation is of the same magnitude as the experimental uncertainty in the determination of the correlation Mach number in these tests, it is not possible to use these data in devising a basis for predicting M_k.

NACA airfoil section	α_m (deg)	M_k	M_β calculated	$M_k - M_\beta$	Reference	Figure
0006	0	0.888	0.845	0.043	4	2
0009	↓	.863	.798	.065	↓	↓
0012	↓	.820	.765	.055	↓	↓
0015	↓	.805	.742	.063	↓	↓
0015	↓	.795	.742	.053	5	↓
0018	↓	.774	.702	.072	4	↓

NACA airfoil section	α_m (deg)	M_k	M_β calculated	$M_k - M_\beta$	Reference	Figure
64_1-206	-2	0.885	0.790	0.095	8	3
64_1-208	↓	.861	.770	.091	↓	↓
64_1-210		.841	.750	.091		
64_1-212		.830	.730	.100		
65_1-208		.867	.769	.098		
65_1-210		.853	.755	.098		
65_1-212		.828	.730	.098		
66_1-206		.888	.812	.076		
66_1-208		.867	.785	.082		
66_1-210		.855	.768	.087	↓	↓
23009		.868	.796	.072	6	4
23012		.839	.757	.082	↓	↓
23015	↓	.804	.727	.077	↓	↓

The supercritical drag rise of an airfoil section at any angle of attack differing significantly from α_m might be expected to be less rapid than that at α_m since the supersonic regions on the upper and lower surfaces do not develop simultaneously. Data for the previously considered groups of airfoil sections at angles of attack greater than α_m are presented in figures 5, 6, 7, and 8. In each figure the data for the various thickness-chord ratios appear to define a single curve For all moderate angles of attack the curves for the NACA 00XX airfoil sections are similar to those for the NACA 230 series. In order to illustrate this similarity the same curve (differing slightly from the curve in fig. 5) has been plotted in figures 6 and 8. The data for the NACA 6-series airfoils for the two moderate angles of attack define one curve which differs from that for the NACA 00XX and NACA 230-series airfoil sections.

Values of M_k chosen on the basis of the experimental data are presented in the following table:

NACA airfoil section	α_o (deg)	M_k	M_β calculated	$M_k - M_\beta$	Reference	Figure
0006	2	0.860	0.763	0.097	4	6
0009	↓	.853	.733	.120	↓	↓
0012		.804	.706	.098		
0015		.804	.685	.119	↓	
0015		.777	.685	.092	5	
0018	↓	.773	.660	.113	4	↓

NACA airfoil section	α_o (deg)	M_k	M_β calculated	$M_k - M_\beta$	Reference	Figure
0009	4	0.769	0.665	0.104	4	6
0012	↓	.754	.648	.106	↓	↓
0015	↓	.767	.632	.135	↓	
0015	↓	.727	.632	.095	5	
0018	↓	.744	.616	.128	4	↓
23009	0	.836	.742	.094	6	8
23012	↓	.811	.715	.096	↓	↓
23015	↓	.783	.700	.083	↓	↓
23009	2	.775	.677	.098	↓	↓
23012	↓	.762	.655	.107	↓	↓
23015	↓	.737	.650	.087	↓	↓
23009	4	.718	.615	.103	↓	↓
23012	↓	.703	.598	.105	↓	↓
23015	↓	.676	.585	.091	↓	↓
23009	6	.642	.560	.082	↓	↓
23012	↓	.644	.560	.084	↓	↓
23015	↓	.615	.540	.075	↓	↓
64_1-206	0	.885	.794	.091	8	5
64_1-208	↓	.859	.770	.089	↓	↓
64_1-210	↓	.832	.751	.081	↓	↓
64_1-212	↓	.814	.727	.087	↓	↓
65_1-208	↓	.859	.769	.090	↓	↓
65_1-210	↓	.835	.752	.083	↓	↓
65_1-212	↓	.813	.732	.081	↓	↓
66_1-206	↓	.895	.808	.087	↓	↓
66_1-208	↓	.869	.786	.083	↓	↓
66_1-210	↓	.854	.766	.087	↓	↓
64_1-206	2	.817	.750	.067	↓	7
64_1-208	↓	.803	.736	.067	↓	↓
64_1-210	↓	.779	.715	.064	↓	↓
64_1-212	↓	.762	.698	.064	↓	↓
65_1-206	↓	.829	.755	.074	↓	↓
65_1-208	↓	.812	.735	.077	↓	↓
65_1-210	↓	.789	.725	.064	↓	↓
65_1-212	↓	.789	.710	.079	↓	↓
66_1-206	↓	.884	.776	.068	↓	↓
66_1-208	↓	.826	.755	.071	↓	↓
66_1-210	↓	.807	.735	.072	↓	↓
66_1-212	↓	.800	.720	.080	↓	↓

NACA airfoil section	α_o (deg)	M_k	M_β calculated	$M_k - M_\beta$	Reference	Figure
64_1-208	4	0.746	0.690	0.056	8	7
64_1-210	↓	.725	.680	.045	↓	↓
64_1-212		.717	.670	.047		
65_1-208		.760	.695	.065		
65_1-210		.747	.690	.057		
65_1-212		.736	.670	.066		
66_1-210		.764	.700	.064		
66_1-212		.753	.688	.065		

In this table, as in the preceding one, possible systematic trends in $M_k - M_\beta$ are masked by the experimental uncertainty in the determination of the wind-tunnel Mach number at M_k. In particular, note that the difference in $M_k - M_\beta$ for the NACA 0015 airfoil as determined in two wind tunnels is as great as the variation in $M_k - M_\beta$ for the NACA 00XX-series airfoils as determined in one of these wind tunnels.

ANALYSIS OF EXPERIMENTAL LIFT DATA

In figure 9, the variation with Mach number of the normal-force coefficient for the family of symmetrical airfoils of reference 7 at an angle of attack of 4° is presented. The Mach number scale used in figure 9 is such that a linear variation would mean that c_n is proportional to $(1-M^2)^{-1/2}$. These airfoils at this angle of attack are of particular interest because of the unusual coincidence that the drag-divergence Mach number of each is about the same. The curves of c_d versus M are also nearly identical. However, there is considerable difference in the variation of lift coefficient with Mach number. Larger losses in lift occur at supercritical speeds for the thicker sections.

It might be expected that the initial supercritical loss in lift (shock stall) is a direct result of the pressure changes brought about by the development of a local supersonic region on the upper surface of the airfoil. However, in reference 1, it is indicated that the loss in lift is due primarily to changes in the pressure distribution over the lower surface.

In figure 10, a breakdown of the normal-force coefficient for the airfoil sections of figure 9 into the normal-force coefficients of the upper and lower surfaces is presented. These values of single-surface normal-force coefficients were determined from integrations of the pressure distributions of reference 7.

A number of trends are apparent from the data for the normal-force coefficients for the individual surfaces. The development of a supersonic region on the upper surface of the airfoil sections produces little change in the manner in which the upper-surface normal-force coefficient varies with Mach number until a Mach number well beyond that for drag divergence is attained. From the curves for the lower surfaces in figure 10, it may be seen that at about the drag-divergence Mach number there is a change in the slope of the lower-surface normal-force-coefficient variation with $(1-M^2)^{-1/2}$. The slope of the curves, after M_d has been exceeded, varies considerably with thickness-chord ratio.

The variation with Mach number of the upper- and lower-surface normal-force coefficients for three NACA airfoil sections at several angles of attack is presented in figure 11. The airfoil sections are: the NACA 0015, a symmetrical conventional airfoil; the NACA 23015, a forward-cambered conventional airfoil; and the NACA 65_2-215, a = 0.5, a cambered low-drag airfoil. In discussing these data, obtained from reference 5, it is convenient to divide the curves into three groups: (1) Curves for which $\alpha_o \approx \alpha_m$, in which cases supersonic regions develop almost simultaneously on both airfoil surfaces; (2) curves for the upper surface with $\alpha_o < \alpha_m$ or for the lower surface with $\alpha_o > \alpha_m$, on which surfaces, herein termed "subsonic," the velocities remain subsonic for a considerable Mach number increment after supersonic regions develop on the opposite surface; and (3) curves for the upper surface with $\alpha_o > \alpha_m$ or for the lower surface with $\alpha_o < \alpha_m$, on which surfaces, herein termed "supersonic," an extensive supersonic region develops before supersonic velocities are reached on the opposite (subsonic) surface of the airfoil.

For the subsonic surfaces, the variation of normal-force coefficient with Mach number changed markedly in the vicinity of the drag-divergence Mach number. The rate of change of the absolute value of c_n with $(1-M^2)^{-1/2}$ at Mach numbers greater than those for drag divergence was approximately the same for all three airfoils. For the examples treated in this report, this variation of normal-force coefficient was brought about by an almost uniform change of pressure coefficient over the subsonic surface. It is possible that these subsonic-surface pressure changes were caused by velocity increments induced by the large wake which is the concomitant of the rapid drag rise.

For angles of attack differing from α_m by 2° or more, the normal-force coefficients for the supersonic surface varied approximately in accordance with the Prandtl-Glauert rule for Mach numbers up to those for drag divergence. At Mach numbers greater than those for drag divergence there was considerable change, with both airfoil section and angle of attack, in the character of the variation with Mach number of the normal-force-coefficient component for the supersonic surface.

An examination of these data indicates that there are fundamental differences between the variation with $(1-M^2)^{-1/2}$ of the lift contributions of the subsonic and supersonic surfaces of moderately thick airfoils at supercritical Mach numbers. To a first approximation, the lift contribution of the subsonic surface appears to be primarily a function of thickness-chord ratio; whereas the contribution of the supersonic surface depends on airfoil shape and angle of attack. Thus, in a theoretical analysis of the supercritical lift characteristics of moderately thick airfoils it might be advantageous to treat the subsonic and supersonic surfaces separately. For the five NACA 00XX airfoil sections, at equal angle of attack and with essentially identical variations of drag coefficient with Mach number, the magnitude of the adverse effect of the lift variation on the subsonic surface decreases with decreasing thickness-chord ratio. Hence, for sufficiently thin sections the influence of the airfoil subsonic surface on supercritical lift characteristics may become of only secondary importance so that transonic similarity rules could be expected to apply.

CONCLUDING REMARKS

By the use of a form of the transonic similarity parameter which correlated the critical Mach numbers of NACA 00XX airfoil sections at zero angle, it was possible to correlate the supercritical drag data for this family to within the experimental accuracy. The excellence of this correlation of the drag data was attributed to the fact that the critical Mach numbers were correlated; however, for an arbitrary family of airfoils, this would not generally be the case unless synthetic forms of the similarity parameters were used. The other type of correlation examined in this report is, in essence, drag (rather than drag coefficient) rise as a function of supercritical Mach number increment. The major experimental uncertainty in such data obtained in a wind tunnel is in the Mach number increment introduced by the presence of the wake which, for a fixed ratio of airfoil chord to wind-tunnel depth, is dependent on drag. (See reference 9.) Thus insofar as the present correlation compares equal values of drag, it may circumvent a major source of error in these wind-tunnel data. For the airfoils considered, there is an essentially unique shape of the drag-rise curve when the angle of attack is that for maximum drag-divergence Mach number. The primary effect of changing the airfoil shape apparently is to change the Mach number at which the drag rise begins.

The portion of the study devoted to lift-coefficient variation with Mach number was limited to a consideration of several airfoil sections for which high-speed pressure distributions were available. One of the most significant observations to be made regarding these data is that, at moderate angles of attack and in the range of Mach numbers for which supersonic flow occurred over only one surface of the airfoil, there

appeared a marked change in the rate of variation with $(1-M^2)^{-1/2}$ of normal-force coefficient of the opposite surface soon after the drag-divergence Mach number was exceeded. This change was most abrupt for the thicker airfoil sections studied and was the primary cause of loss in lift at supercritical speeds. Insofar as this trend is related to pressure changes induced by the wake, application to airfoil lift characteristics of a transonic theory which neglects viscosity would be expected to be successful only for relatively thin airfoil sections.

Ames Aeronautical Laboratory
National Advisory Committee for Aeronautics
Moffett Field, Calif., April 10, 1952

REFERENCES

1. Nitzberg, Gerald E., and Crandall, Stewart: A Study of Flow Changes Associated with Airfoil Section Drag Rise at Supercritical Speeds. NACA TN 1813, 1949.

2. von Kármán, Theodore: The Similarity Law of Transonic Flow. Jour. Math. and Physics, vol. 26, no. 3, Oct. 1947, pp. 182-190.

3. Busemann, Adolf: Application of Transonic Similarity. NACA TN 2687, 1952.

4. Göthert, B.: Profilmessungen im DVL Hochgeschwindigkeits-windkanol (2.7 M) Zentrale für Wissenschaftliches Berichtswesen der Luftfahrtforschung, (Berlin-Adlershof) FB 1490. (Available as Nat. Res. Lab. Tech. Trans. TT-31, Ottawa, Canada, Sept. 6, 1947.)

5. Graham, Donald J., Nitzberg, Gerald E., and Olson, Robert N.: A Systematic Investigation of Pressure Distributions at High Speeds Over Five Representative NACA Low-Drag and Conventional Airfoil Sections. NACA Rep. 832, 1945. (Formerly NACA RM A7B04 and MR A5K20a)

6. Göthert, B.: Hochgeschwindigkeitsmessungen an Profilen der Reihe NACA 230 mit verschiedenen Dickenverhaltnissen, Zentrale für Wissenschaftliches Berichtswesen der Luftfahrtforschung, UM 1259/1-3. (Berlin-Adlershof), 1944. (Available as British trans., Ministry of Aircraft Production. Volkenrode. Repts. and Trans. 409a, 409b, and 409c. High-Speed Measurements on Sections of Series NACA 230 with Different Thickness Ratios. May, 1946.)

7. Göthert, B.: Druckverteilungs - und Impulsverlustschaubilder für das Profil NACA 00XX -1.10 bei hohen Unterschallgeschwindigkeiten, Zentrale für Wissenschaftliches Berichtswesen der Luftfahrtforschung, FB Nr. 1505/1-5. (Berlin-Adlershof), 1941. (Available as Canadian trans., Nat. Res. Labs., Div. of Mech. Eng., Tech. Trans. TT-25, TT-26, TT-27, TT-28, and TT-29. Pressure Distribution and Momentum Loss Diagrams for the NACA Profile 0 00 XX - 1.1 30 at High Subsonic Speed. May 9, 1947.)

8. Van Dyke, Milton D.: High-Speed Subsonic Characteristics of 16 NACA 6-Series Airfoils. NACA TN 2670, 1951.

9. Allen, H. Julian, and Vincenti, Walter G.: Wall Interference in a Two-Dimensional-Flow Wind Tunnel, with Consideration of the Effect of Compressibility. NACA Rep. 782, 1944. (Formerly NACA ARR 4K03)

10. Feldman, F.: Untersuchung von Symmetrischen Tragflugelprofilen bei hohen Unterschallgeschwindigkeiten in einem Geschlossenen Windkanal. Mitteilungen aus dem Institut für Aerodynamik, Heft Nr. 14, Zurich 1948.

11. Thom, A.: Blockage Corrections in a Closed High-Speed Tunnel. R&M No. 2033 British, A.R.C., 1943.

12. Allen, H. Julian, and Nitzberg, Gerald E.: The Effect of Compressibility on the Growth of the Laminar Boundary Layer on Low-Drag Wings and Bodies. NACA TN 1255, 1947.

13. Abbott, Ira H., von Doenhoff, Albert E., and Stivers, Louis S., Jr.: Summary of Airfoil Data. NACA Rep. 824, 1945. (Formerly NACA ACR L5C05)

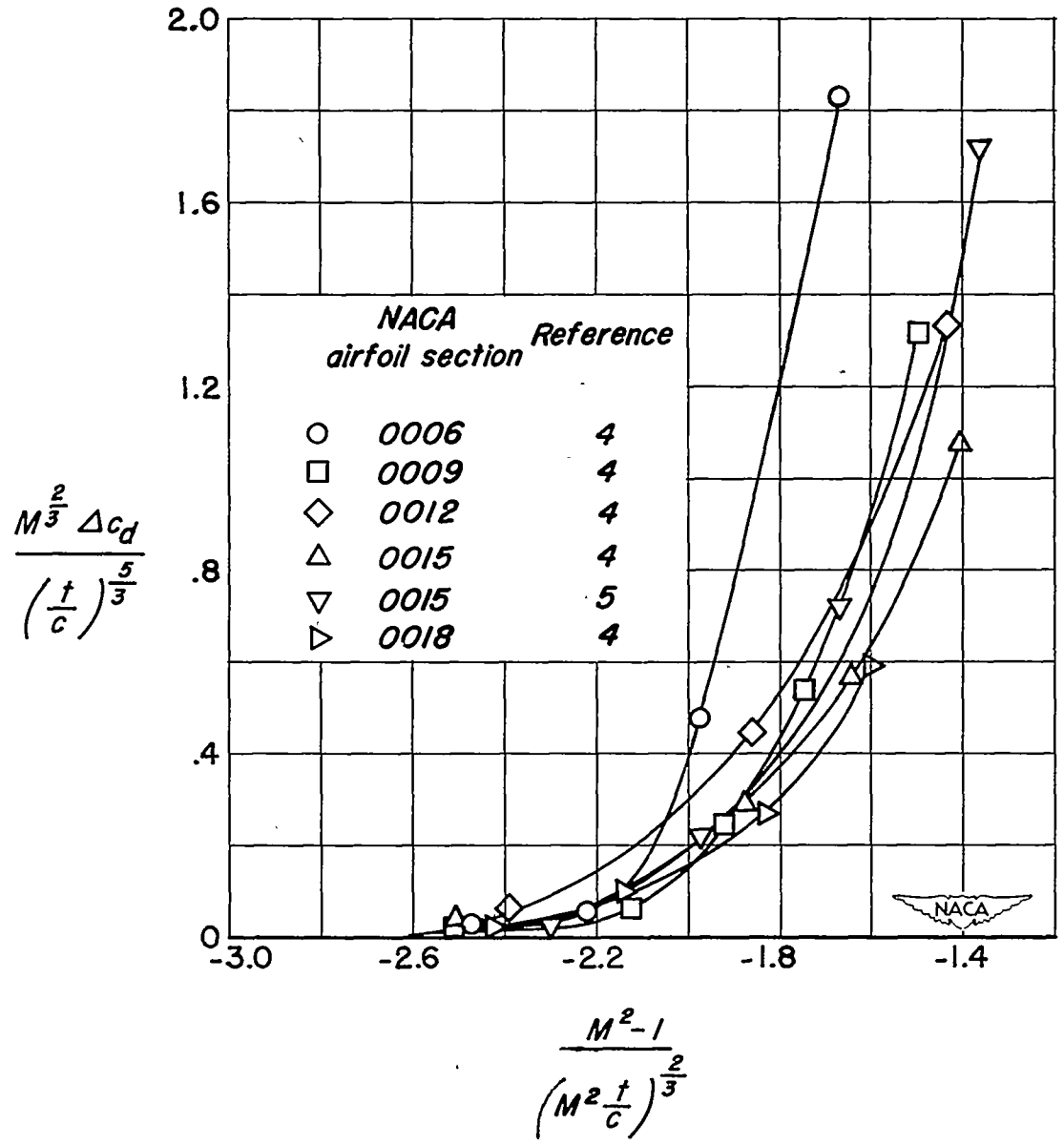

Figure 1.– Correlation of pressure-drag coefficient in terms of transonic-similarity-rule parameters for several NACA 00XX airfoil sections. Angle of attack, 0°.

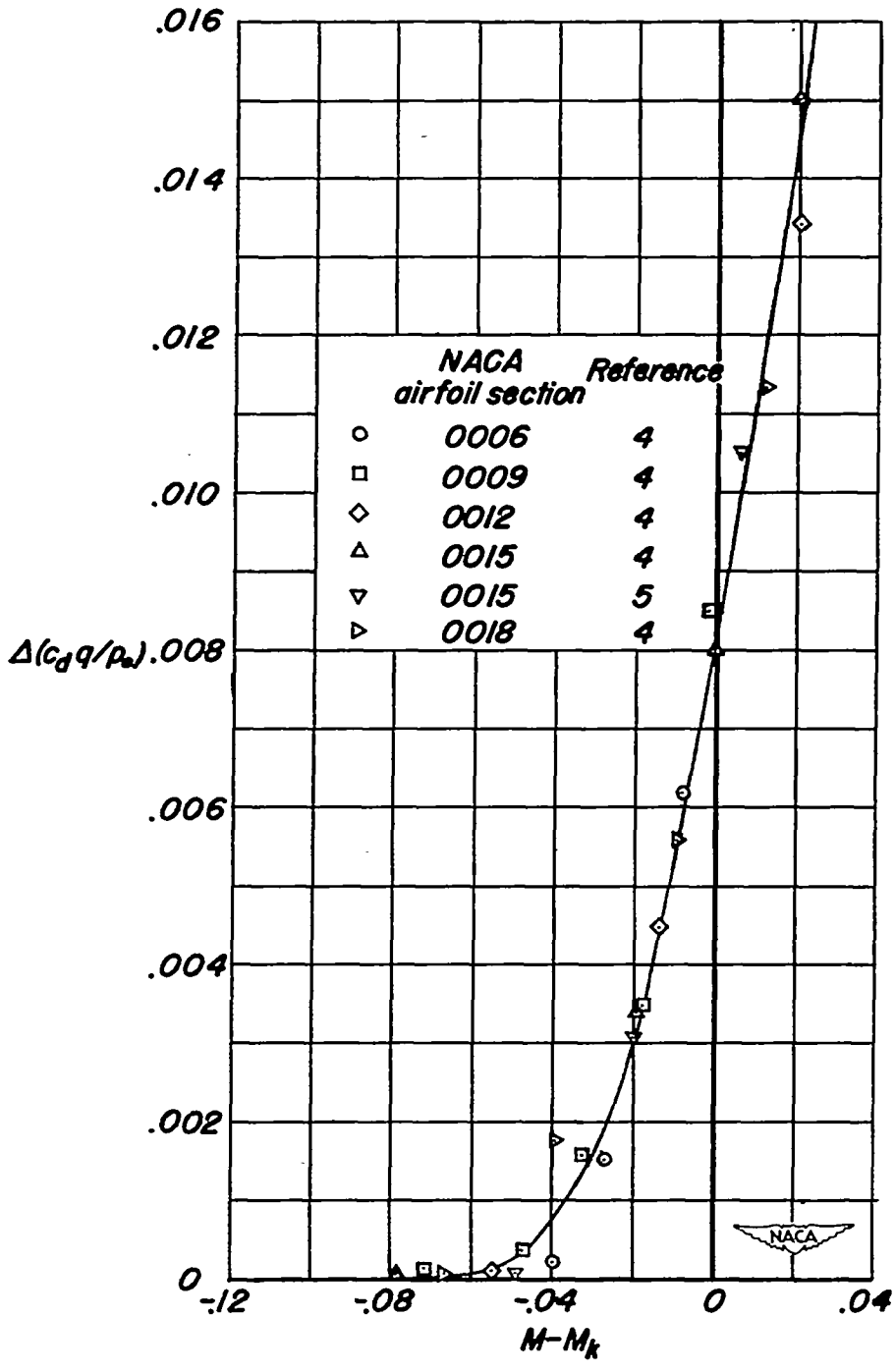

Figure 2.– Correlation of pressure-drag coefficient for several NACA 4-digit series airfoil sections. Angle of attack, 0°.

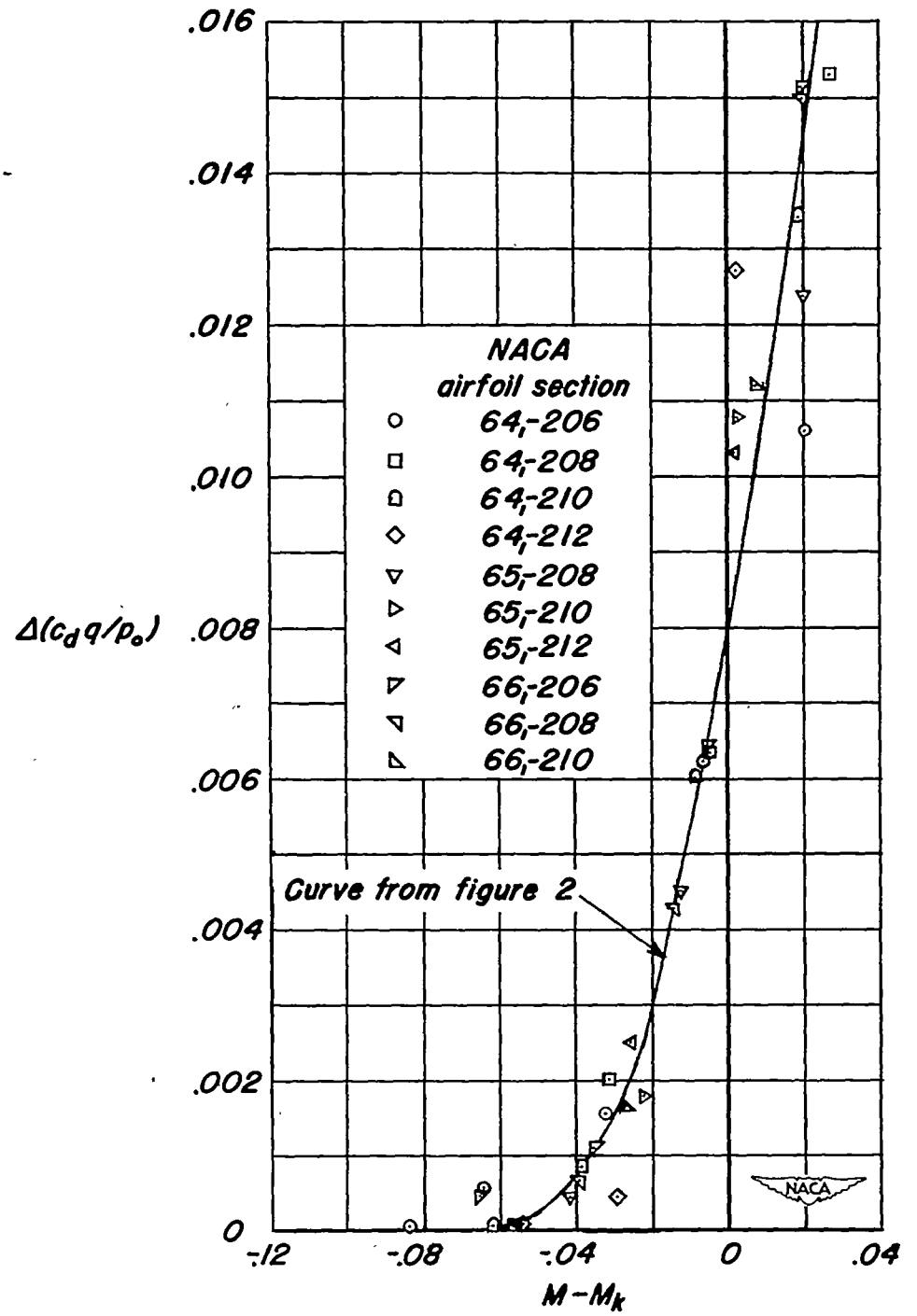

Figure 3.- Correlation of pressure-drag coefficient for several NACA 6-series airfoil sections. Angle of attack, -2°.

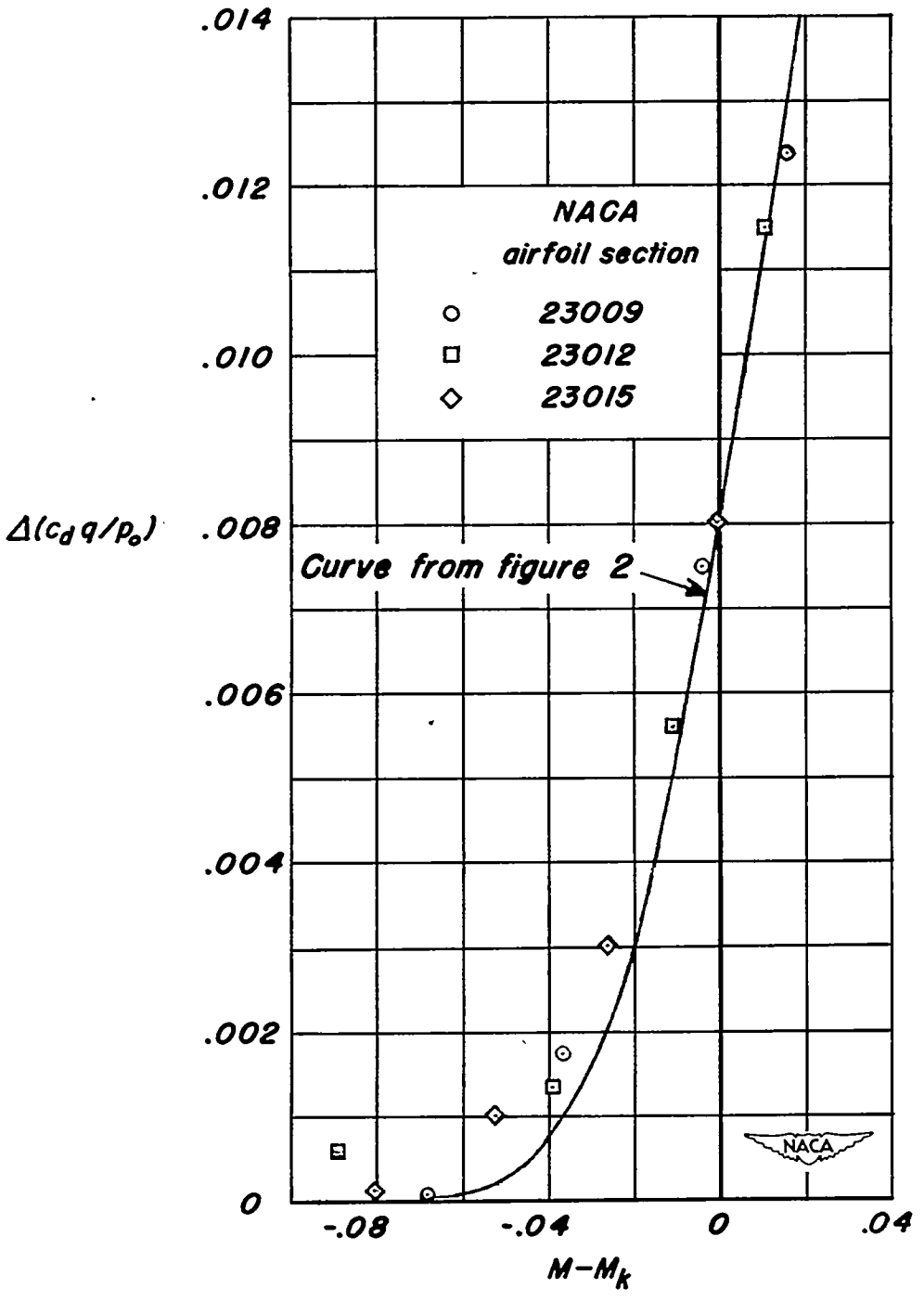

Figure 4.– Correlation of pressure-drag coefficient for several NACA 230-series airfoil sections. Angle of attack, −2°.

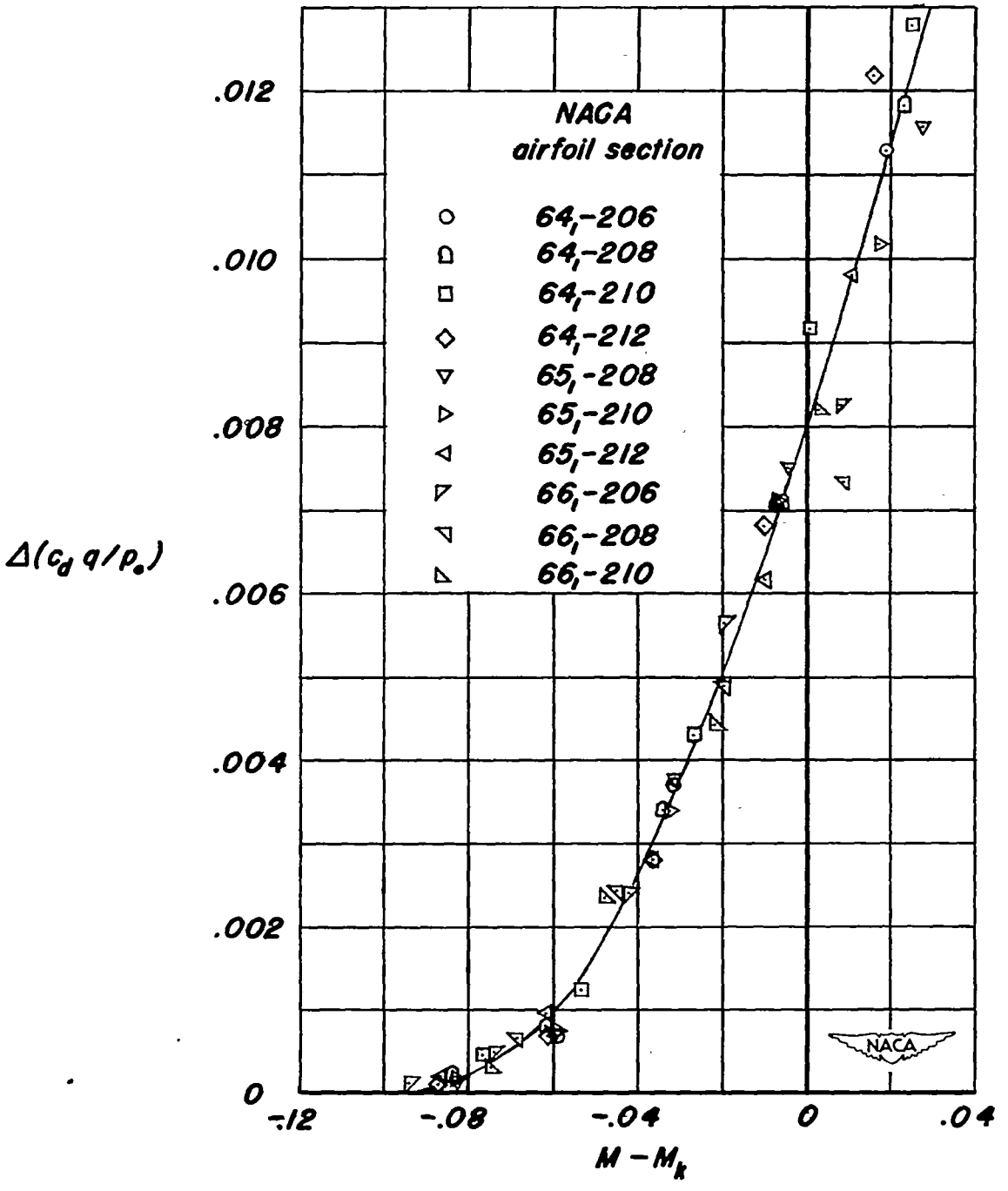

Figure 5.- Correlation of pressure-drag coefficient for several NACA 6-series airfoil sections. Angle of attack, 0°.

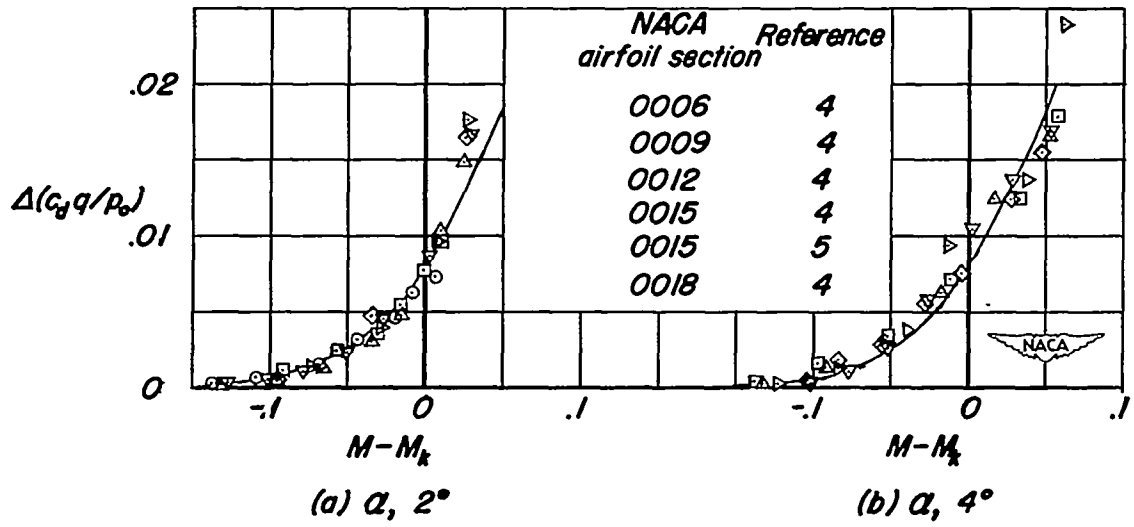

Figure 6.- Correlation of pressure-drag coefficient for several NACA 00XX airfoil sections at various angles of attack.

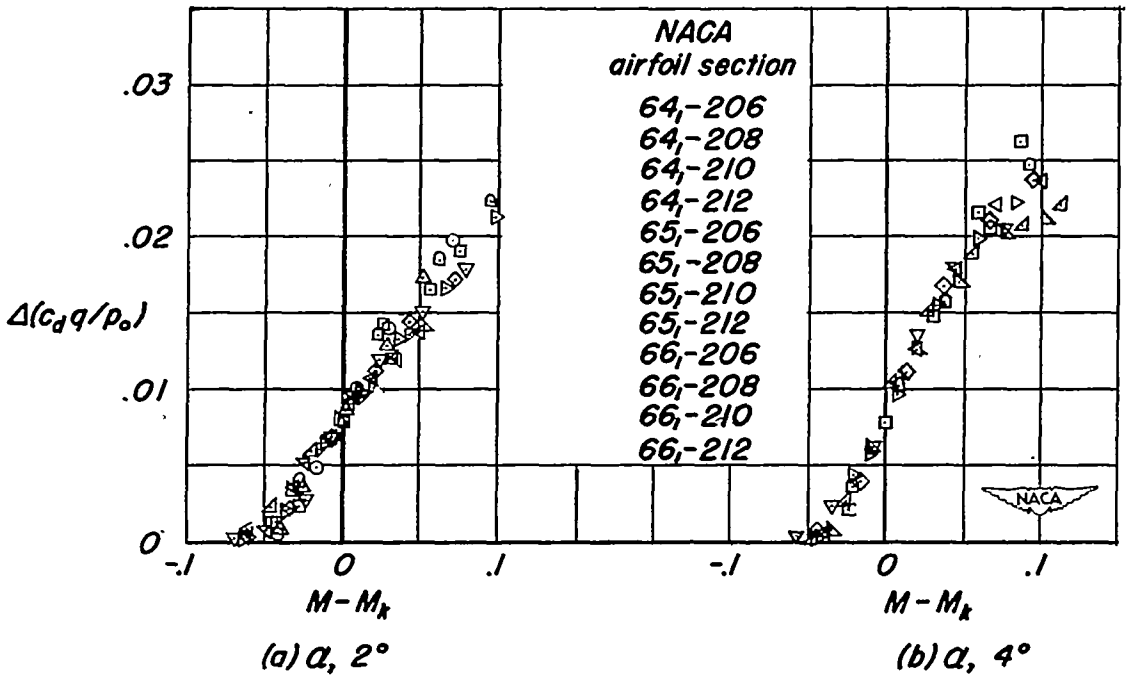

Figure 7.- Correlation of pressure-drag coefficient for several NACA 6-series airfoil sections at various angles of attack.

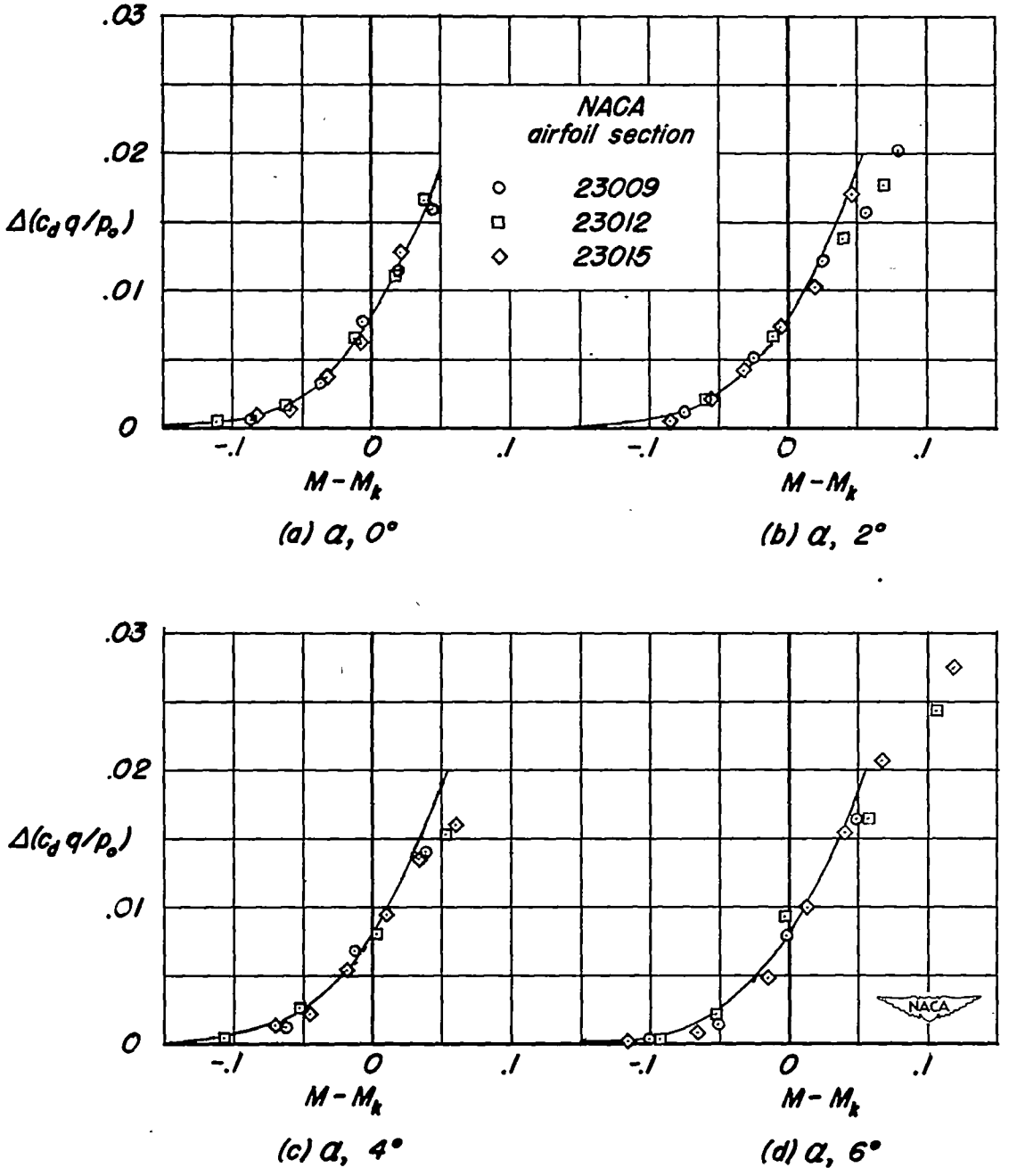

Figure 8.- Correlation of pressure-drag coefficient for several NACA 230-series airfoil sections at various angles of attack.

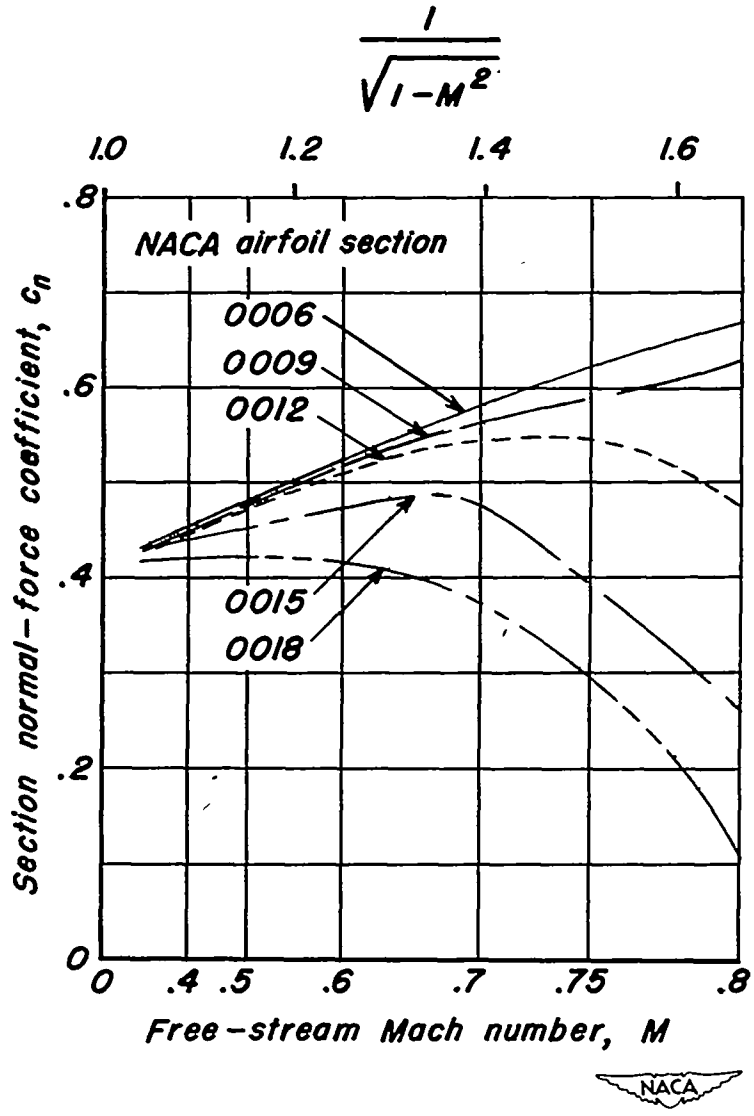

Figure 9.- Variation with free-stream Mach number of section normal-force coefficient for several NACA OOXX airfoil sections at 4° angle of attack.

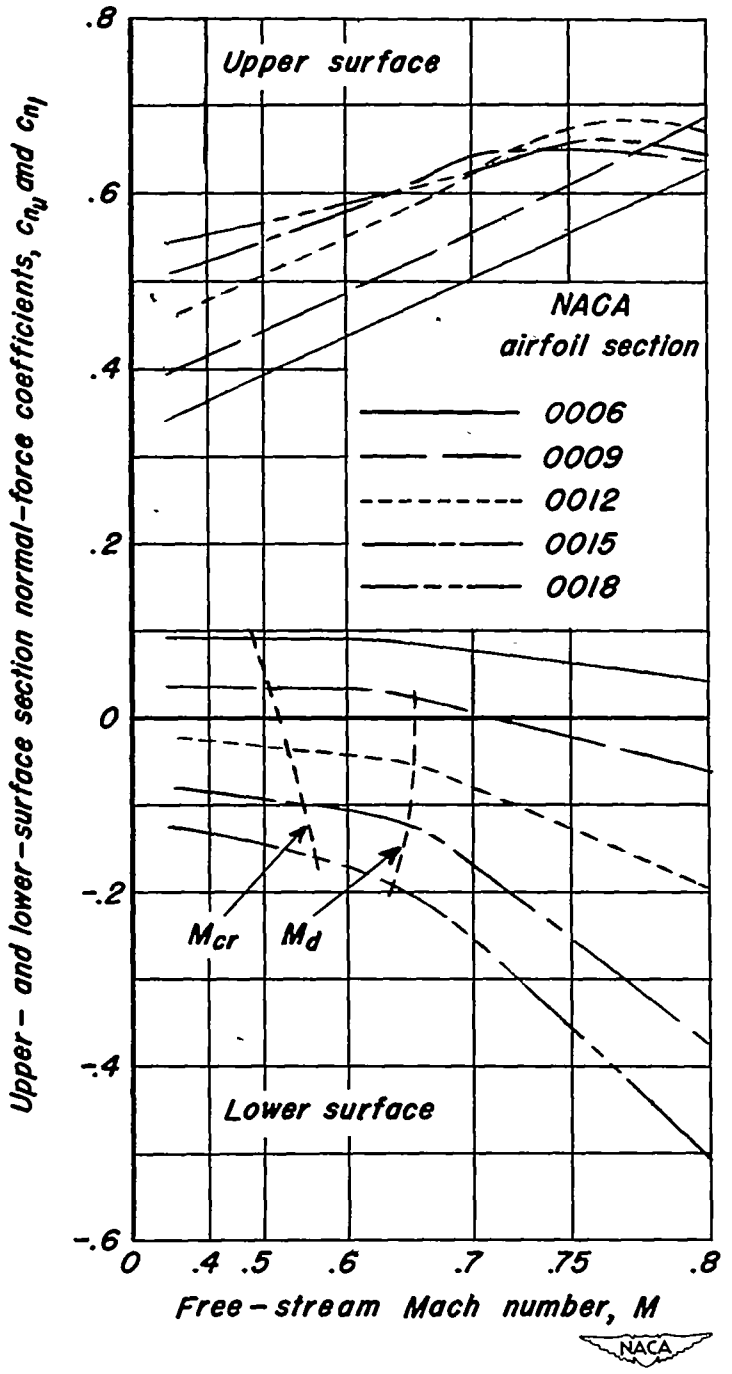

Figure 10.- Variation with free-stream Mach number of upper- and lower-surface normal-force coefficients for several NACA OOXX airfoil sections at 4° angle of attack.

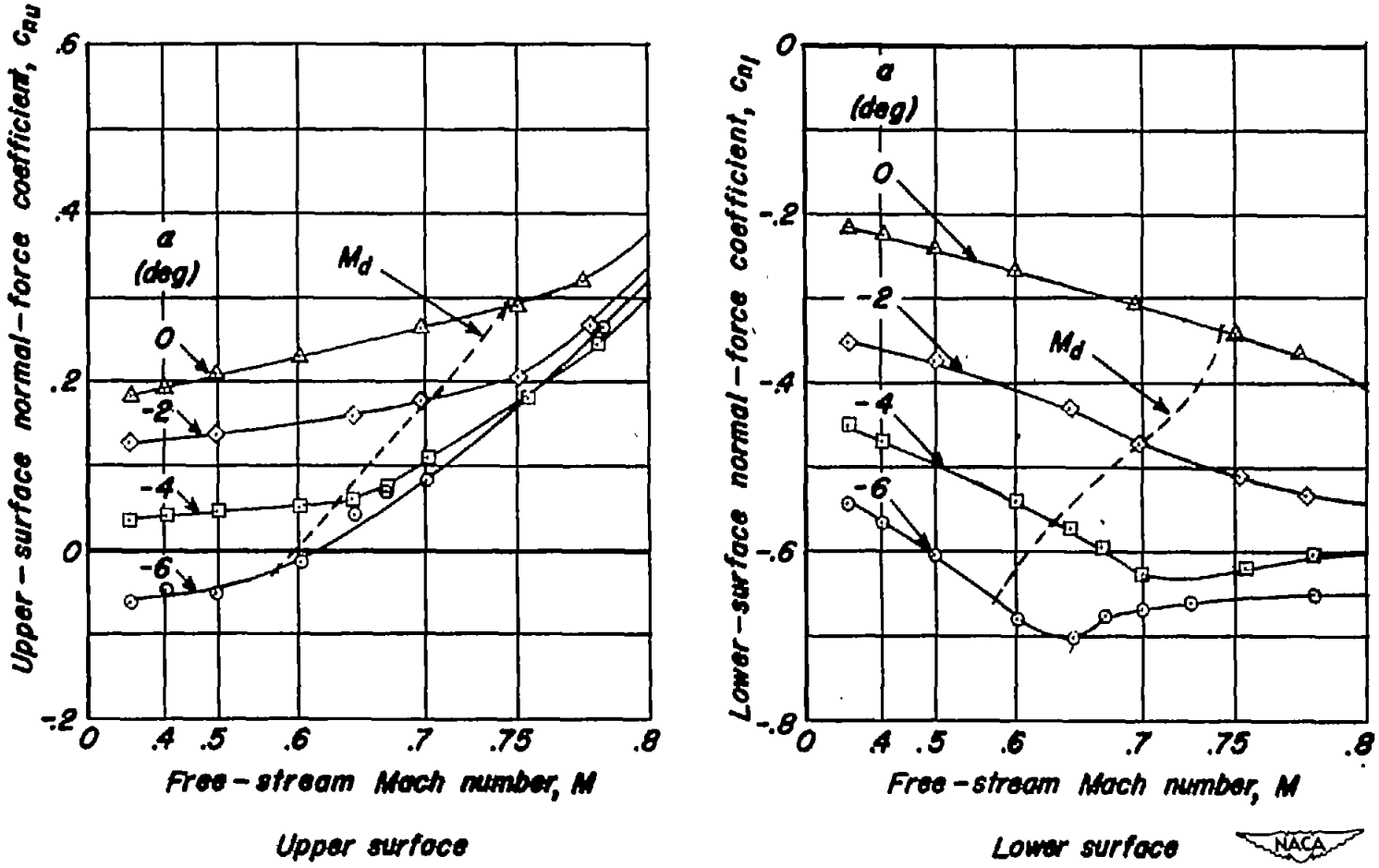

(a) Airfoil section, NACA 0015.

Figure 11.- Variation with free-stream Mach number of upper- and lower-surface normal-force coefficients for several 15-percent-thick NACA airfoil sections at several angles of attack.

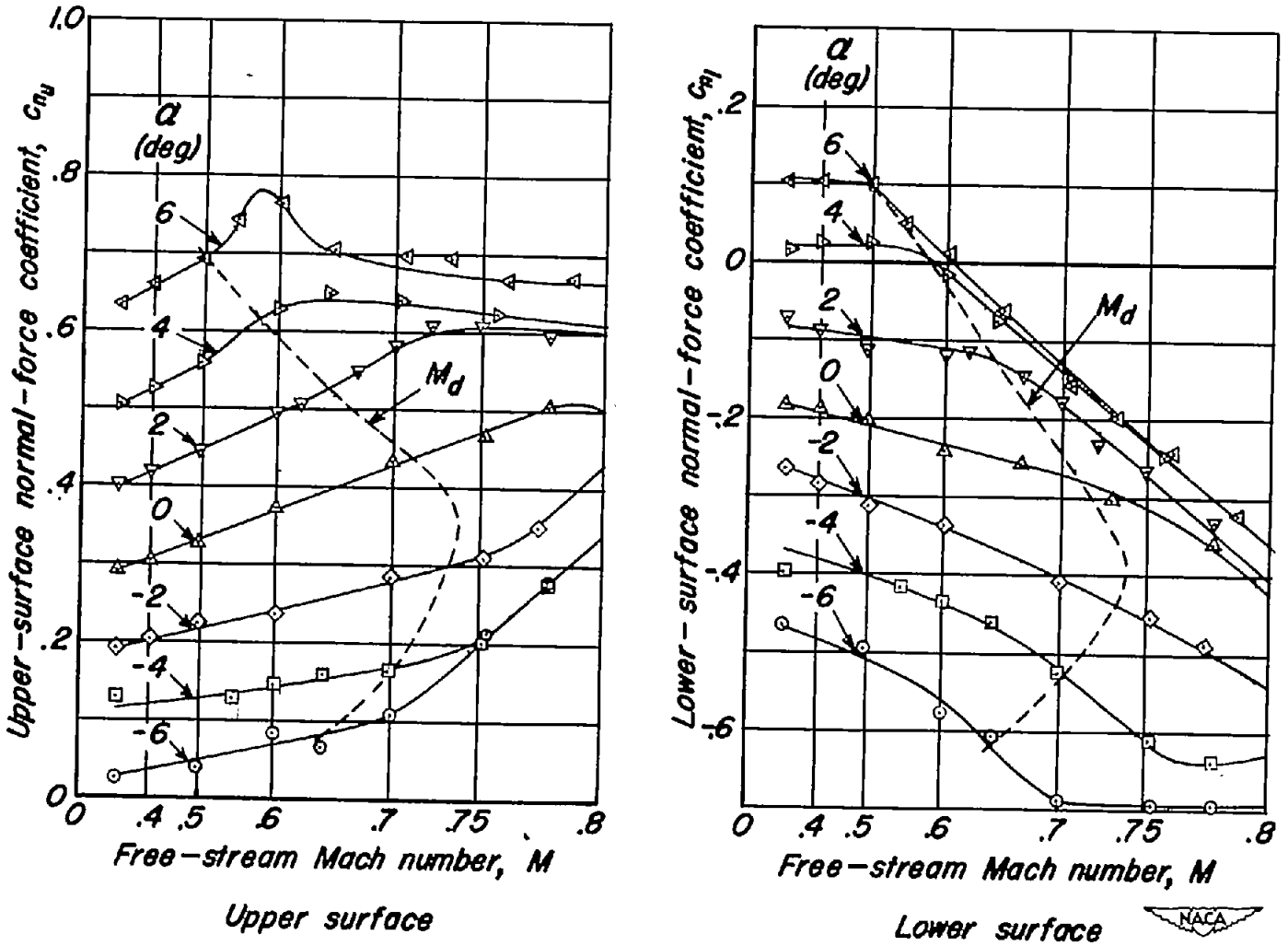

(b) Airfoil section, NACA 23015.

Figure 11.- Continued.

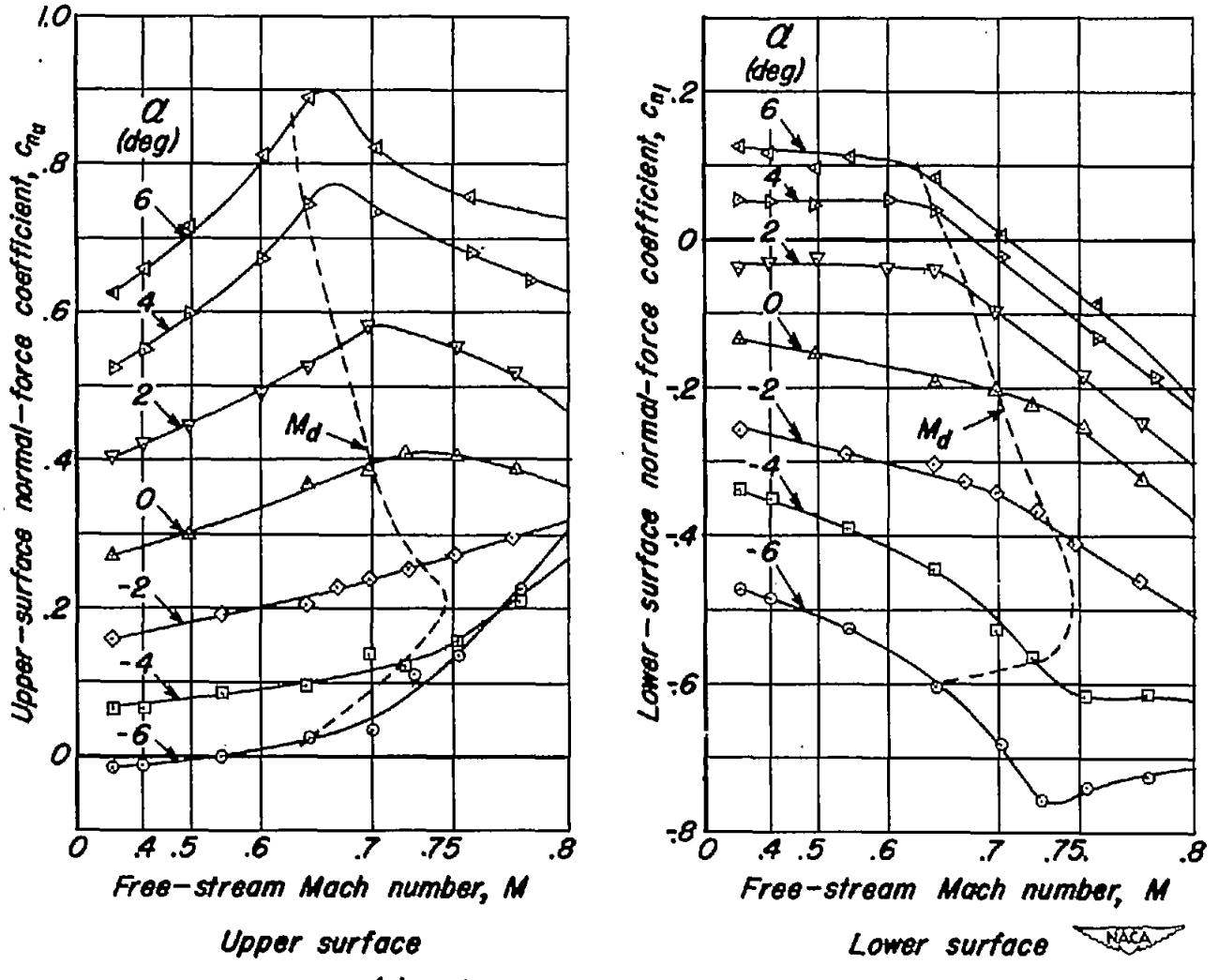

(c) Airfoil section, NACA 65_2-215, a=0.5.

Figure 11.- Concluded.